

RESEARCH ARTICLE

Lipid remodeling and an altered membrane-associated proteome may drive the differential effects of EPA and DHA treatment on skeletal muscle glucose uptake and protein accretion

Stewart Jeromson,¹ Ivor Mackenzie,² Mary K. Doherty,² Phillip D. Whitfield,² Gordon Bell,³ James Dick,³ Andy Shaw,¹ Francesco V. Rao,⁴ Stephen P. Ashcroft,⁵ Andrew Philp,⁵ Stuart D. R. Galloway,¹ Iain Gallagher,¹ and D. Lee Hamilton¹

¹Health and Exercise Sciences Research Group, University of Stirling, Stirling, United Kingdom; ²Department of Diabetes and Cardiovascular Science, University of Highlands and Islands, Inverness, United Kingdom; ³Institute of Aquaculture, University of Stirling, Stirling, United Kingdom; ⁴DC Biosciences, Limited, Dundee Technopole, Dundee, United Kingdom; and ⁵School of Sport, Exercise and Rehabilitation Sciences, University of Birmingham, Birmingham, United Kingdom

Submitted 5 October 2015; accepted in final form 13 June 2017

Jeromson S, Mackenzie I, Doherty MK, Whitfield PD, Bell G, Dick J, Shaw A, Rao FV, Ashcroft SP, Philp A, Galloway SD, Gallagher I, Hamilton DL. Lipid remodeling and an altered membrane-associated proteome may drive the differential effects of EPA and DHA treatment on skeletal muscle glucose uptake and protein accretion. *Am J Physiol Endocrinol Metab* 314: E605–E619, 2018. First published June 27, 2017; doi:10.1152/ajpendo.00438.2015.—In striated muscle, eicosapentaenoic acid (EPA) and docosahexaenoic acid (DHA) have differential effects on the metabolism of glucose and differential effects on the metabolism of protein. We have shown that, despite similar incorporation, treatment of C₂C₁₂ myotubes (CM) with EPA but not DHA improves glucose uptake and protein accretion. We hypothesized that these differential effects of EPA and DHA may be due to divergent shifts in lipidomic profiles leading to altered proteomic profiles. We therefore carried out an assessment of the impact of treating CM with EPA and DHA on lipidomic and proteomic profiles. Fatty acid methyl esters (FAME) analysis revealed that both EPA and DHA led to similar but substantial changes in fatty acid profiles with the exception of arachidonic acid, which was decreased only by DHA, and docosapentaenoic acid (DPA), which was increased only by EPA treatment. Global lipidomic analysis showed that EPA and DHA induced large alterations in the cellular lipid profiles and in particular, the phospholipid classes. Subsequent targeted analysis confirmed that the most differentially regulated species were phosphatidylcholines and phosphatidylethanolamines containing long-chain fatty acids with five (EPA treatment) or six (DHA treatment) double bonds. As these are typically membrane-associated lipid species we hypothesized that these treatments differentially altered the membrane-associated proteome. Stable isotope labeling by amino acids in cell culture (SILAC)-based proteomics of the membrane fraction revealed significant divergence in the effects of EPA and DHA on the membrane-associated proteome. We conclude that the EPA-specific increase in polyunsaturated long-chain fatty acids in the phospholipid fraction is associated with an altered membrane-associated proteome and these may be critical events in the metabolic remodeling induced by EPA treatment.

cell signaling; fish oil; fatty acid; insulin; lipidomics; lipids

FATTY ACIDS play an important role in skeletal muscle metabolism, not only as substrates for oxidative phosphorylation or vital structural components of membranes but also as regulators of enzyme activities and signaling molecules (8). Furthermore, dysfunctions in the control of fatty acid metabolism can be an important factor in the etiology of conditions such as insulin resistance and muscle atrophy (8). The lipid composition of skeletal muscle undergoes constant fluctuations and is reflective of dietary fat intake (6). There is strong evidence to suggest that the enrichment of skeletal muscle with omega-3 (n-3) fatty acids may have therapeutic benefits on muscle metabolism and function (14). Oral n-3 supplementation above the Reference Dietary Intake is known to result in significant incorporation of n-3 fatty acids into the skeletal muscle lipid pool (6, 13, 30).

Several n-3 supplementation studies in humans have observed beneficial effects ranging from an increased sensitivity to anabolic stimuli (43, 44) and muscle function (40, 45). Eight weeks of n-3 supplementation improved the muscle protein synthetic response to a hyperinsulinaemic amino acid infusion in both young (44) and elderly individuals (43). Furthermore, when taken alongside a resistance-based exercise program (12, 40) or in the absence of any strength training (45) n-3 fatty acids enhance strength and or physical function in the elderly. Concurrent with anabolic properties, n-3 fatty acids also display anticatabolic effects. n-3 Supplementation prevented muscle mass losses in burned guinea pigs (5) and protected against muscle mass loss during antineoplastic therapy in cancer patients (34). However, when combined in systematic reviews, n-3 fatty acids do not always show a beneficial effect on muscle mass during cancer treatment (39). Moreover, n-3 fatty acids attenuated soleus atrophy in rodents that underwent 10 days of hindlimb immobilization (55).

As well as effects on muscle protein metabolism there is building evidence to suggest that n-3 fatty acids may also modulate glucose metabolism. Current meta-analyses detect a neutral or small effect of n-3 fatty acids on measures of insulin sensitivity (4). However, there are several studies across a range of models utilizing higher doses of n-3s that support a role for n-3s in improving muscle mitochondrial function and

Address for reprint requests and other correspondence: D. L. Hamilton, Health and Exercise Sciences Research Group, Univ. of Stirling, Stirling, UK FK9 4LA (e-mail: d.l.hamilton@stir.ac.uk).

glucose metabolism (23, 28, 35, 37, 47, 48). For instance, replacing 3.4% of the kilocalories with n-3 fatty acids on a high-fat diet protects mice against declines in glucose tolerance during a 10-wk high-fat diet despite similar increases in body weight compared with high fat alone (28). Whereas supplementation studies in humans have not demonstrated a consensus (4), an interesting lipid infusion trial has shown n-3 fatty acids to be bioactive in humans with respect to glucose metabolism (46). More specifically, the addition of n-3 fatty acids to a lipid infusion of n-6 fatty acids attenuated the decline in insulin-stimulated glucose disposal caused by n-6 infusion alone, suggesting that the n-3 fatty acids have a protective effect on glucose metabolism in the presence of an n-6 overload (46).

Fish oil and n-3 supplements are a heterogeneous mixture of fatty acids of which eicosapentaenoic acid (EPA, 20:5) and docosahexaenoic acid (DHA, 22:6) are thought to be the most biologically active. Due to many studies using a combination of EPA and DHA and varying ratios of each fatty acid, it is difficult to assert whether EPA or DHA alone is causing the observed effects or if EPA and DHA work synergistically or antagonistically for that matter. The molecular mechanisms of n-3 action are still poorly understood. Work from the laboratory of Olefsky et al. (37) suggests that GPR120 acts as a general n-3 receptor in macrophages and adipocytes that, when activated by n-3 fatty acids, leads to increases in whole body insulin sensitivity by reducing inflammation. EPA has also been shown to antagonize the action of TNF- α on C₂C₁₂ myotube formation in a manner partially dependent on peroxisome proliferator-activated receptor- γ (PPAR γ) (29). Additionally, EPA reduces the activation of nuclear factor- κ B (NF- κ B), leading to a reduction in muscle RING finger protein-1 (Murf-1) signaling, an important mediator of muscle atrophy in cultured myotubes (22). Furthermore, a follow-up study employing both EPA and DHA demonstrated that DHA was more efficient in this mechanism than EPA (52). However, EPA has been shown to improve metabolic flexibility in response to changing substrate availabilities (21). EPA has also previously been shown to improve both basal and insulin-stimulated glucose uptake in cultured myotubes (1). However, it remains to be seen whether DHA similarly improves glucose uptake in skeletal muscle. Despite the numerous similar intracellular effects and similar structure, EPA and DHA may have divergent physiological effects in skeletal muscle. EPA improves skeletal muscle protein metabolism while DHA has a nonsignificant effect (24). In other striated muscle models such as cardiomyocytes, EPA but not DHA increases glucose and fatty acid uptake despite similar effects on cell signaling (18). In plasma, both EPA and DHA reduced triacylglycerol (TAG), but only DHA modulates high-density lipoprotein (HDL) and low-density lipoprotein (LDL) particle size (53). Collectively, these data suggest that in certain contexts, EPA and DHA can have differential biological effects.

The molecular mechanisms underpinning the divergent physiological effects of EPA vs. DHA are currently underexplored. However, differential remodeling of the lipid profile may partially explain the divergent physiological response observed between EPA and DHA. Currently, studies attempting to address how n-3 fatty acids affect the lipidomic profile of skeletal muscle are limited. As expected, n-3 intake leads to incorporation into the lipid pool of multiple tissues, i.e.,

plasma, muscle, adipose tissue, and liver with a significant proportion being directed toward phospholipid pools (7, 27, 30, 42–44). This incorporation is not limited to the plasma membrane and is also incorporated into subcellular organelles such as mitochondria (20). It is hypothesized that a primary driver of the effects of EPA and DHA is the displacement of arachidonic acid (AA) from membranes with studies from a range of models supporting this (27, 32, 42) while some *in vivo* human studies observe no change in total AA in the skeletal muscle lipid pool (30). However, this does not discount the possibility that AA might be displaced from specific lipid fractions. Multiple human studies have assessed the impact of n-3 supplementation on skeletal muscle phospholipid pool; however, the use of a heterogeneous mix of n-3 fatty acids precludes the ability to detect the isolated effects of EPA vs DHA on lipid profiles (6, 13, 30). Furthermore, into which skeletal muscle phospholipid fractions EPA and DHA are incorporated are poorly understood. In plasma phospholipids, EPA and DHA induce a similar lipid profile yet EPA increased docosapentaenoic acid (DPA 22:5 n-3) and a differential but nonsignificant increase in stearate acid (SA 18:0) (31). In smooth muscle cell phospholipids, both EPA and DHA are heavily incorporated into the phosphatidylcholine (PC) fraction but EPA is divergently incorporated into the phosphatidylinositol (PI) and phosphatidylserine (PS) fraction while DHA is incorporated into the phosphatidylethanolamine (PE) fraction (33).

One of the main cellular fates for fatty acids is incorporation into complex lipid species, and therefore, it seems logical to hypothesize that the differential action of EPA and DHA may be due to differential effects on the cellular lipidome. To date, no study has characterized the impact of EPA and DHA individually on lipidomic profiles in skeletal muscle. In this article, we demonstrate that the C₂C₁₂ cell line acts as a model in which EPA and DHA have differential effects on metabolism. We followed these experiments by an extensive assessment of lipid changes, hypothesizing that the divergent effects of EPA and DHA are associated with differential regulation of the skeletal muscle lipidome. The lipidomic profiling indicated that multiple membrane-associated lipid species were differentially altered by EPA and DHA treatments. We therefore hypothesized that the lipidomic remodeling would be associated with remodeling of the membrane-associated proteome. Stable isotope labeling by amino acids in cell culture (SILAC)-based proteomics of the membrane fraction indicated EPA and DHA differentially regulate the membrane-associated proteome. Therefore, the effects of EPA may be due to membrane-associated proteomic remodeling secondary to lipidomic remodeling of the membrane-associated lipids.

MATERIALS AND METHODS

Materials. All plasticware for tissue culture was purchased from Fisher Scientific (Loughborough, UK). Tissue culture media and sera were purchased from Invitrogen. Fatty acids EPA and DHA (>99%, liquid form) were purchased from Sigma-Aldrich (Dorset, UK). 2-deoxy-D-[³H]glucose (2-DG) was purchased from Hartman Analytic. All solvents were liquid chromatography-mass spectrometry (LC-MS) grade (Fisher Scientific).

Cell culture. C₂C₁₂ myoblasts were grown in DMEM containing 20% fetal bovine serum and 1% penicillin/streptomycin and incubated at 37°C and 5% CO₂. Myoblasts were maintained at ~60% confluence. Differentiation was induced once confluence reached 80–90%

by changing the media to differentiation media (DM; DMEM supplemented with 2% horse serum and 1% penicillin/streptomycin) for 72 h. Following 72-h differentiation, cells were treated with 50 μ M EPA or 50 μ M DHA prebound to 2% fatty acid free (FAF)-BSA for 72 h before collection. As a control, cells were treated with 2% FAF-BSA for 72 h before collection. Fatty acids were conjugated to 2% FAF-BSA in DM by constant agitation for 1 h at 37°C. Following treatment, cell pellets were collected following three washes in 2% FAF-BSA in PBS and centrifuged at 800 rpm for 4 min, excess liquid was removed, and pellets were frozen in liquid nitrogen and stored at -80°C until further analysis.

Fatty acid methyl esters analysis. Total lipids were extracted by homogenizing in 20 vol of chloroform/methanol (2:1 vol/vol). Total lipids were prepared according to the method of Folch et al. (17) and nonlipid impurities were removed by a wash with 0.88% (wt/vol) KCl. The weight of lipids was determined gravimetrically after evaporation of solvent and overnight desiccation under vacuum. Fatty acid methyl esters (FAME) were prepared by acid-catalyzed transesterification of total lipids according to the method of Christie (8a). Extraction and purification of FAME was performed as described by Ghioni et al. (18a). FAME were separated by gas-liquid chromatography using a ThermoFisher Trace GC 2000 (ThermoFisher, Hemel Hempstead, UK) equipped with a fused silica capillary column (ZB-Wax, 60 \times 0.25- μ m \times 0.25-mm inner diameter; Phenomenex, Macclesfield, UK) with hydrogen as carrier gas and using on-column injection. The temperature gradient was from 50 to 150°C at 40°C/min and then to 195°C at 1.5°C/min and finally to 220°C at 2°C/min. Individual methyl esters were identified by reference to published data (2a). Data were collected and processed using the Chromcard for Windows (version 2.00) computer package (Thermoquest Italia, Milan, Italy). All experiments were carried in duplicate from four independent experiments. Data were represented as fold-change from the respective BSA control condition and logged to log₂, and significance was determined by *t*-test and corrected for false discovery rate.

Global lipidomic analysis of C₂C₁₂ myotubes. Lipid extraction was performed according to the method described above. The lipids were analyzed by LC-MS using a Thermo Exactive Orbitrap mass spectrometer (Thermo Scientific), equipped with a heated electrospray ionization probe and coupled to a Thermo Accela 1250 UHPLC system. All samples were analyzed in both positive and negative ion mode over the mass to charge (*m/z*) range 200–2,000. The lipids were separated on to a Thermo Hypersil Gold C18 column (1.9 μ m, 2.1 \times 100 mm). Mobile phase A consisted of water containing 10 mM ammonium formate and 0.1% (vol/vol) formic acid. Mobile phase B consisted of 90:10 isopropanol/acetonitrile containing 10 mM ammonium formate and 0.1% (vol/vol) formic acid. The initial conditions for analysis were 65% A/35% B. The percentage of mobile phase B was increased to 100% over 10 min and held for 7 min before reequilibration with the starting conditions for 4 min. The raw LC-MS data were processed with Progenesis QI v2.0 software (Nonlinear Dynamics, Newcastle, UK) and searched against LIPID MAPS (www.lipidmaps.org) and the Human Metabolome Database (<http://www.hmdb.ca/>) for identification. All experiments were carried out in duplicate from three independent experiments.

Phospholipid profiling of C₂C₁₂ myotubes. To assess the incorporation of EPA and DHA into cellular phospholipids, the lipid extracts from C₂C₁₂ myotubes were analyzed by electrospray ionization-tandem mass spectrometry (ESI-MS/MS). All analyses were performed using a Thermo TSQ Quantum Ultra triple quadrupole mass spectrometer equipped with a heated electrospray ionization probe. Samples were directly infused into the ion source at a flow rate of 5 μ l/min. PC, lysophosphatidylcholine (LPC), and sphingomyelin species were identified by precursor scanning for mass to charge ratio (*m/z*) 184 in positive ion mode. PE and lysophosphatidylethanolamine (LPE) species were identified by neutral loss scanning for *m/z* 141 in positive ion mode. Phosphatidylserine species were identified by neutral loss scanning for *m/z* 87 in negative ion mode. Phosphatidyl-

inositol species were identified by precursor scanning for *m/z* 241 in negative ion mode. The data are expressed as a percentage composition of the relevant phospholipid fraction.

Glucose uptake. C₂C₁₂ myotubes were exposed to 50 μ M EPA or 50 μ M DHA prebound to 2% FAF-BSA or 2% FAF-BSA as a control for 48 h before a 2 h serum-starve. Following the 2-h serum starve cells were exposed to insulin (100 nmol/l) or vehicle control for 30 min. Myotubes were incubated (12 min) with 10 μ mol/l 2-DG (24.4 kBq/ml; Hartman Analytic) at 20°C. Nonspecific uptake was determined using 10 μ mol/l cytochalasin B (Sigma-Aldrich). After lysis, cell-associated radioactivity was measured (Beckman, High Wycombe, UK; LS 6000IC scintillation counter), and protein was quantified using the Bradford reagent. Data represented are the average of six independent experiments carried out in duplicate.

Mitochondrial function. C₂C₁₂ myotubes, were exposed to 50 μ M EPA or 50 μ M DHA prebound to 2% FAF-BSA or 2% FAF-BSA as a control for 48 h. Following 48 h in the respective treatments, cells were degassed and exposed to a mito-stress test in a Seahorse cellular respiration analyzer as previously described (16).

Muscle protein synthesis and muscle protein breakdown. Protein degradation was assessed by the quantification of the released L-[2,4,³H] phenylalanine into the culture media. Following 4 days of differentiation, myotubes were incubated with medium containing 2.5 μ Ci L-[2,4,³H]phenylalanine/ml and the label was maintained for 24 h to label long-lived proteins. Following the pulse, the cells were washed two times in PBS and incubated in cold chase media (DMEM + 2 mM L-phenylalanine) for 3 h to allow for degradation of short-lived proteins. Myotubes were then treated with either 50 μ M EPA/DHA bound to 2% FAF-BSA or 2% FAF-BSA alone for 24 h. Following treatment, an aliquot of the media was removed and radioactivity released was assessed by scintillation counting. The remaining myotubes were then thoroughly washed with ice-cold saline (0.9%) and lysed with 50 mM NaOH + 1% SDS for a minimum of 30 min at room temperature. Residual radioactivity in cell lysates was then assessed by scintillation counting. Total radioactivity was calculated as the sum of the L-[2,4,³H]phenylalanine released into the media, and the residual cell-retained L-[2,4,³H]phenylalanine. Protein breakdown is presented as the fraction of the total incorporated L-[2,4,³H]phenylalanine released into the media.

Basal protein synthesis was assessed by the incorporation of L-[2,4,³H]phenylalanine into peptide chains. Following differentiation, myotubes were treated with either 50 μ M EPA/DHA bound to 2% FAF-BSA or 2% FAF-BSA alone for 24 h. At the end of the treatment period, the media were removed and DMEM containing 1 μ Ci L-[2,4,³H] phenylalanine (0.5 μ Ci/ml) was added for 180 min. The reaction was stopped by two washes in ice-cold saline (0.9%) before three washes with trichloroacetic acid (10%) to remove any unincorporated tracer. Residual trichloroacetic acid was then removed by rinsing cells with methanol, and the plates were left to dry. Myotubes were then lysed in 50 mM NaOH + 1% SDS for a minimum of 30 min. An aliquot was collected for liquid scintillation counting to assess ³H incorporation into the protein, and the remaining lysate was used to determine protein content by the DC protein assay. Protein synthesis is presented as counts per minute per micrograms of protein.

Protein content. Protein content following 72-h treatment with 50 μ M EPA or 50 μ M DHA prebound to 2% FAF-BSA or 2% FAF-BSA as a control was determined by multiplying the concentration of the supernatant [as determined using the bicinchoninic acid protein assay according to the manufacturer's instructions; Sigma-Aldrich] by the total volume of supernatant collected from a six-well plate. Data are representative of five independent experiments carried out in triplicate.

Cell processing. Cell lysates were collected from six-well plates by scraping on ice in RIPA buffer [50 mmol/l Tris-HCl pH 7.5, 50 mmol/l NaF, 500 mmol/l NaCl, 1 mmol/l sodium vanadate, 1 mmol/l EDTA, 1% (vol/vol) Triton X-100, 5 mmol/l sodium pyrophosphate,

0.27 mmol/l sucrose, and 0.1% (vol/vol) 2-mercaptoethanol and Complete protease inhibitor cocktail (Roche)] followed by snap freezing on liquid nitrogen. For preparation for Western blotting samples were thawed and debris was removed by centrifugation at 4°C for 15 min at 13,000 *g*. The supernatant was then removed, and protein concentration was determined using the bicinchoninic acid protein assay according to the manufacturer's instructions (Sigma-Aldrich).

Western blot analysis. For Western blotting, 100 µg of supernatant were made up in Laemmli sample buffer, and 15 µg of total protein was loaded per well and run at 150 V for 1 h 15 min. Proteins were then transferred onto Whatman Immunobilon Nitrocellulose membranes (Fisher Scientific, Loughborough, UK) at 30 V overnight on ice. Membranes were blocked in 3% BSA-Tris-buffered saline (containing vol/vol 0.1% Tween 20) for 1 h at room temperature, followed by incubation in primary antibodies [PKBthr308 (no. 2965) or total PKB (no. 4691) GLUT 1 (sc-7903; Santa Cruz Biotechnology), GLUT4 (no. 2213S), hexokinase 1 (no. 2204S), hexokinase 2 (no. 2867S), and Mito profile (Abcam; no. ab110413) (New England Biolabs unless stated)] at 4°C overnight. Membranes underwent three 5-min washes in TBS-Tween followed by incubation in the appropriate secondary antibodies [secondary horseradish peroxidase-conjugated antibody was purchased from Abcam (no. 6721)] for 1 h at room temperature. Membranes were again washed three times for 5 min followed by incubation in enhanced chemiluminescence reagent (Bio-Rad, Herts, UK). A Bio-Rad ChemiDoc was used to visualize and quantify protein expression. Phospho-PKB was normalized to the corresponding total protein. Data are representative of three independent experiments carried out in duplicate.

Membrane proteome. Proteins associated with membranes were assessed using the SILAC proteomic method (38). C₂C₁₂ myoblasts were grown in DMEM supplemented with 20% dialyzed (10 kDa) fetal bovine serum plus labeled amino acids lysine and arginine in a humidified atmosphere of 37°C and 5% CO₂. Cells intended to act as the control group were grown in with unlabeled lysine and arginine (light), the EPA treatment group were grown in R6K4 media [L-arginine-13C6 hydrochloride and L-lysine-4,4,5,5-d4 hydrochloride (medium)], while the DHA treatment group were grown with R10K8 containing media [L-arginine-13C6, 15N4 hydrochloride, and L-lysine-13C6,15N2 hydrochloride (heavy)]. The use of combined labeled arginine and lysine ensures that nearly all peptides will contain a label after tryptic digestion. Cells were allowed to grow for at least six population doublings to ensure full incorporation of labeled amino acids. We observed that use of dialysed sera and labeled media did not affect doubling time, cell morphology, or differentiation capacity. Upon reaching 90–100% confluence, the media were replaced with DMEM containing 2% dialyzed donor horse serum (10 kDa) to induce differentiation. After 3–4 days of differentiation, myotubes were treated with either control, 50 µM EPA, or 50 µM DHA for 72 h. For membrane proteome analysis, membranes were isolated using the Thermo Scientific Mem-PER Plus protein membrane extraction kit. The membrane proteome was assessed by LC-MS/MS.

Mass spectrometry. The resulting peptides were fractionated using an Ultimate 3000 nano HPLC system in line with an Orbitrap Fusion Tribrid mass spectrometer (Thermo Scientific). In brief, peptides in 1% (vol/vol) formic acid were injected onto an Acclaim PepMap C18 nano-trap column (Thermo Scientific). After being washed with 0.5% (vol/vol) acetonitrile, 0.1% (vol/vol), formic acid peptides were resolved on a 250 mm × 75-µm Acclaim PepMap C18 reverse phase analytical column (Thermo Scientific) over a 150-min organic gradient, using seven gradient segments (1–6% solvent B over 1 min, 6–15% B over 58 min, 15–32% B over 58 min, 32–40% B over 5 min, 40–90% B over 1 min, held at 90% B for 6 min, and then reduced to 1% B over 1 min) with a flow rate of 300 nl/min. Solvent A was 0.1% formic acid, and solvent B was aqueous 80% acetonitrile in 0.1% formic acid. Peptides were ionized by nano-electrospray ionization at 2.0 kV using a stainless steel emitter with an internal diameter of 30 µm (Thermo Scientific) and a capillary temperature of 275°C.

All spectra were acquired using an Orbitrap Fusion Tribrid mass spectrometer controlled by Xcalibur 2.1 software (Thermo Scientific) and operated in data-dependent acquisition mode. FTMS1 spectra were collected at a resolution of 120,000 over a scan range (*m/z*) of 350–1,550, with an automatic gain control target of 300,000 and a maximum injection time of 100 ms. Precursors were filtered using an intensity range of 1E4 to 1E20 and according to charge state (to include charge states 2–6) and with monoisotopic precursor selection. Previously interrogated precursors were excluded using a dynamic window (40 s ± 10 ppm). The MS2 precursors were isolated with a quadrupole mass filter set to a width of 1.4 *m/z*. ITMS2 spectra were collected with an automatic gain control target of 20,000, maximum injection time of 40 ms, and collision-induced dissociation collision energy of 35%.

Quantification and bioinformatics analysis. The raw mass spectrometric data files obtained for each experiment were collated into a single quantitated data set using MaxQuant (version 1.2.2.5) (10) and Andromeda search engine software (11). Enzyme specificity was set to that of trypsin, allowing for cleavage NH₂-terminal to proline residues and between aspartic acid and proline residues. Other parameters used were as follows: 1) variable modifications, methionine oxidation, protein *N*-acetylation, gln → pyro-glu, Phospho(STY); 2) fixed modifications, cysteine carbamidomethylation; 3) database: target-decoy human MaxQuant (ipi.HUMAN.v3.68); 4) heavy labels: R6K4 and R10K8; 5) MS/MS tolerance: FTMS: 10 ppm, ITMS: 0.6 Da; 6) maximum peptide length, 6; 7) maximum missed cleavages, 2; 8) maximum of labeled amino acids, 3; and 9) false discovery rate, 1%. Peptide ratios were calculated for each arginine- and/or lysine containing peptide as the peak area of labeled arginine/lysine divided by the peak area of nonlabeled arginine/lysine for each single-scan mass spectrum. Peptide ratios for all arginine and lysine containing peptides sequenced for each protein were averaged. Data are normalized using 1/median ratio value for each identified protein group per labeled sample.

Statistics. Statistical analyses were carried out in Graphpad Prism with ANOVA followed by Tukey's honestly significant difference test. For FAME analyses, data were assessed in R statistical packages and tested by *t*-test and corrected by false discovery rate. Statistical significance was determined with a *P* < 0.05. The global lipidomic data sets were subjected to principal component analysis (PCA) and orthogonal projection latent structure-discriminant analysis (OPLS-DA) with Pareto scaling using SIMCA-P v13.0 software (Umetrics, Umea, Sweden). The OPLS-DA models were validated by using the internal cross-validation function. Membrane protein abundance was considered altered if fold-change was <0.75 or >1.25. Enrichment of biological processes was determined using gene ontology, using the whole genome of *Mus musculus* as a background reference list.

RESULTS

EPA and DHA substantially increase the abundance of omega-3 species but have differential effects on individual omega-3 fatty acids. After exposure to 50 µM EPA or DHA for 72 h, C₂C₁₂ myotubes were collected for FAME analysis to determine lipid profiles. EPA and DHA significantly increased total omega-3 fatty acid content from baseline values (EPA, 951 ± 81%, *P* = 0.0014; DHA, 750 ± 56%, *P* = 0.0009) with no significant difference detected between EPA and DHA treatment (*P* = 0.115; Fig. 1). The changes in omega-3 abundance are a result of differential shifts in specific omega-3 fatty acids caused by EPA or DHA treatment. The increase in omega-3 content by DHA is a result of accumulation of mainly DHA (22:6 n-3, 3,050% ± 310%; see Fig. 5). While, incubation of myotubes with EPA results in the accumulation of EPA (20:5 n-3, 1,630 ± 23.38%) and DPA (22:5 n-3, 1,318 ±

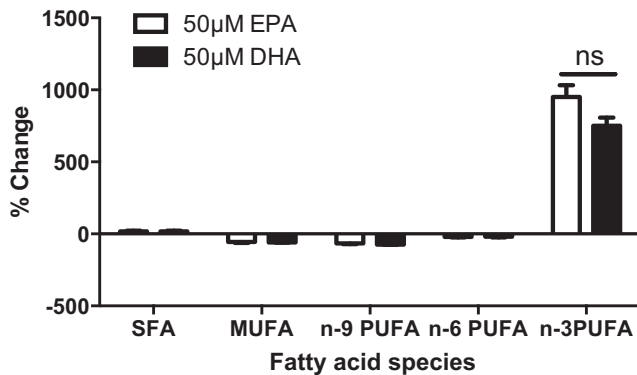


Fig. 1. Eicosapentaenoic acid (EPA) and docosahexaenoic acid (DHA) enhance n-3 content to a similar degree. C_2C_{12} myotubes were incubated in either 2% fatty acid free (FAF)-BSA or 2% FAF-BSA preincubated to 50 μ M EPA or 50 μ M DHA for 72 h. Fatty acid analysis was carried out by fatty acid methyl esters (FAME) analysis ($n = 4$ in duplicate), and data are presented as % change from BSA control grouped by fatty acid species. SFA, saturated fatty acids; MUFA, monounsaturated fatty acids; n-9 PUFA, omega-9 polyunsaturated fatty acids; n-6 PUFA, omega-6 polyunsaturated fatty acids; n-3 PUFA, omega-3 polyunsaturated fatty acids.

199.8%; see Fig. 5). These data suggest that EPA is elongated to DPA while DHA remains largely unmodified.

EPA and DHA have differential effects on skeletal muscle glucose uptake. Insulin-stimulated 2-DG uptake was determined after 48 h in either EPA or DHA. EPA treatment

significantly increased both basal and insulin-stimulated 2-DG uptake indicating that EPA treatment increases the capacity for glucose uptake (Fig. 2A). DHA did not have any significant effects on 2-DG uptake (Fig. 2A). The observed changes in 2-DG uptake did not appear to be related to any change in insulin-stimulated PKB phosphorylation as phospho-blot analysis revealed that insulin-stimulated PKB phosphorylation was the same between treatments and controls (Fig. 2B). In addition, EPA/DHA treatment did not appear to affect GLUT1 or GLUT4 expression (Fig. 2C) nor did it appear to affect the expression of hexokinase 1 or hexokinase 2 (Fig. 2D).

EPA and DHA treatment does not alter mitochondrial respiration. As no changes in glucose transporters were detected, we next assessed whether changes in mitochondrial oxygen consumption may explain the increase in glucose uptake following EPA treatment. C_2C_{12} myotubes were treated with 50 μ M EPA or DHA for 24 h. Following treatment, multiple inhibitors/uncouplers (oligomycin, FCCP, and rotenone/anitmycin A) were used to probe various parameters of mitochondrial function using the Seahorse XF mito stress test. A two-way ANOVA found a significant interaction between oxygen consumption and inhibitor compound, indicating the successful manipulation of mitochondrial function (Fig. 3A). However, fatty acid treatment did not lead to changes in cellular oxygen consumption on any parameter measured (Fig. 3A). Consistent with the lack of changes in mitochondrial function, there were no alterations in the abundance of ATP

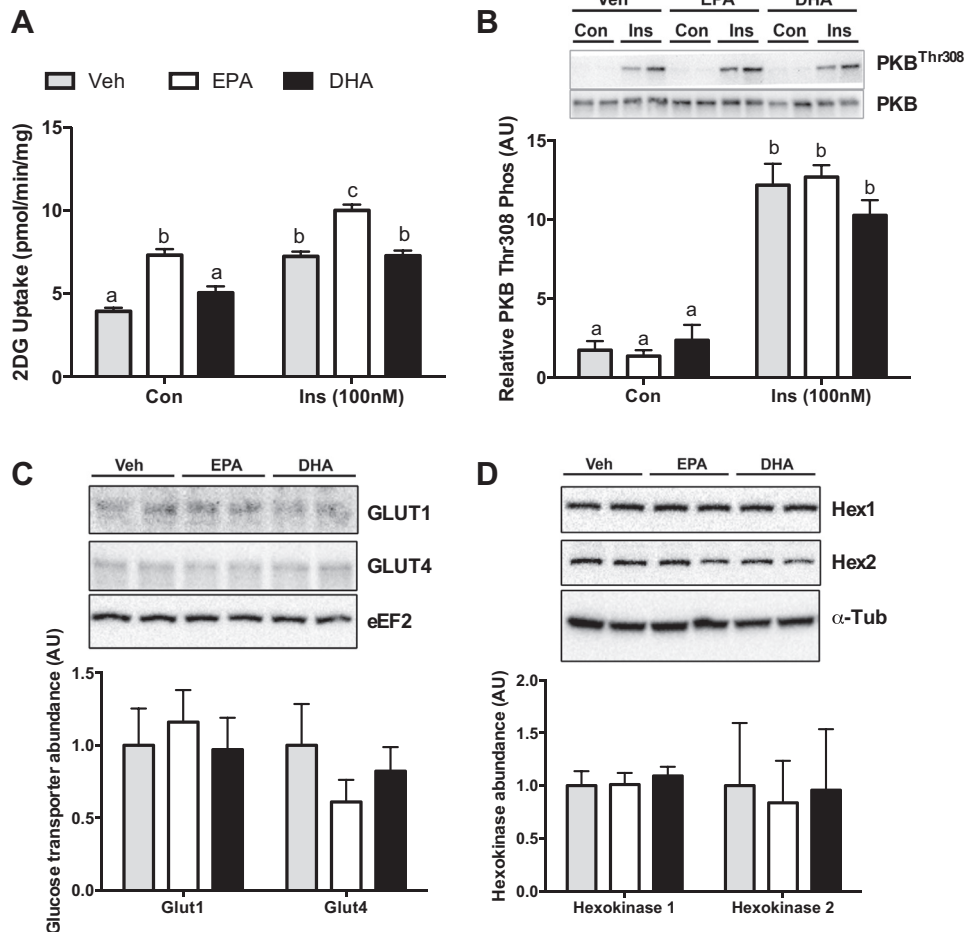


Fig. 2. EPA and DHA have differential effects on C_2C_{12} glucose uptake independently of changes in PKB Thr308 phosphorylation or GLUT1/4 and hexokinase1/2 expression. Glucose uptake was determined using a radiolabeled 2-deoxy-glucose uptake assay ($n = 6$ in duplicate; A), and PKB Thr308 phosphorylation ($n = 4$ in duplicate; B) was determined using SDS-PAGE and phospho-specific antibodies, the signal for which was normalized to t-PKB expression (*inset*: representative blots). 2-DG, 2-deoxy-D- $[^3H]$ glucose; AU, arbitrary units. GLUT1/4 expression (C) was normalized to t-eEF2, while hexokinase1/2 expression (D) was normalized to α -tubulin. Bars not connected by the same letter are significantly different from each other ($P < 0.05$).

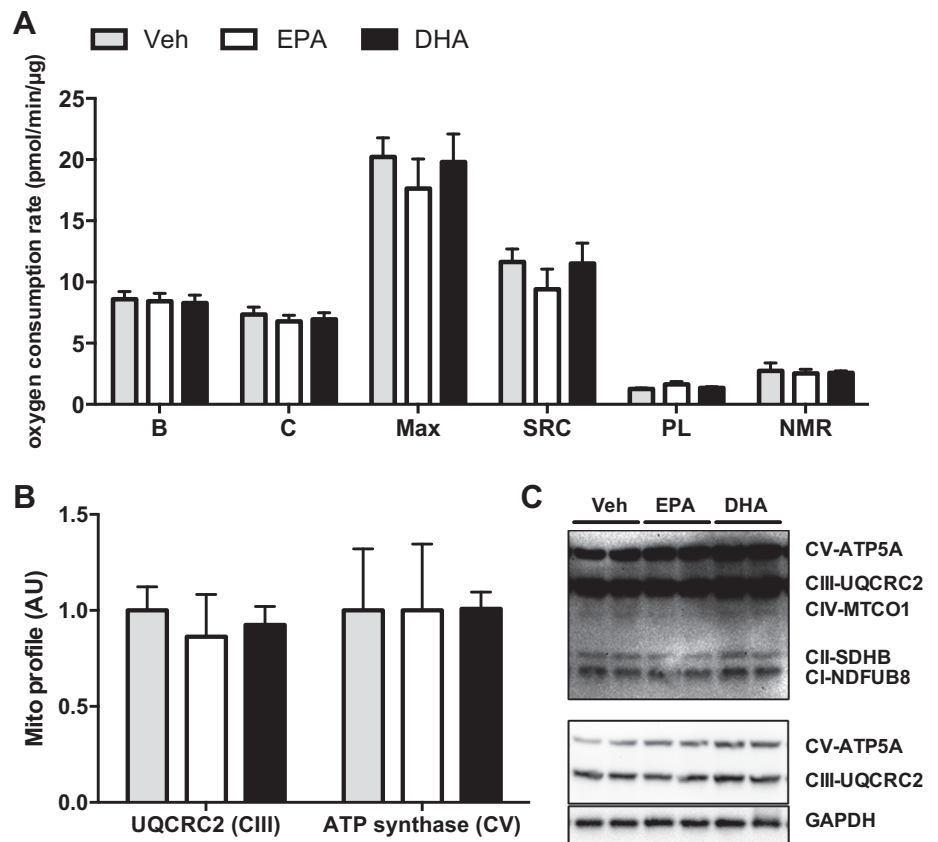


Fig. 3. EPA and DHA treatment do not modulate mitochondrial function or mitochondrial protein expression. C₂C₁₂ myotubes were incubated in either 2% FAF-BSA or 2% FAF-BSA preincubated to 50 μ M EPA or 50 μ M DHA for 48 h. *A*: 1 set of myotubes was exposed to a mitochondrial stress test in the Seahorse XFA and oxygen consumption was assessed. *B*, baseline; *C*, coupled; NMR, non-mitochondrial respiration; SRC, spare respiratory capacity; Max, maximal respiration; PL, proton leak. *B*: parallel set of myotubes were collected for Western blot analysis of mitochondrial protein expression with the mito-blot. *C*: representative blots.

synthase and UQCRC2 (complex V and complex III, respectively; Fig. 3, *B* and *C*).

EPA enhances protein accretion through a reduction in protein breakdown while DHA has a neutral effect. After a 72-h incubation with EPA or DHA, myotubes were collected to determine total protein content. When myotubes were incubated with EPA, total protein content was enhanced while incubation with DHA had a neutral effect (Fig. 4*C*). Protein balance is determined by the balance between synthesis and breakdown of proteins. Thus the observed protein accretion may be reflected in changes in either protein synthesis or breakdown. To understand the mechanisms underlying the changes in protein content, we directly assessed protein synthesis and breakdown and related signaling processes. Neither fatty acid had any effect on basal protein synthesis after a 24-h incubation (Fig. 4*A*). Anabolic signaling assessed by the phosphorylation status of mammalian target of rapamycin, P70S6K1, and 4E-BP1 was not different between groups, corresponding with lack of changes in protein synthesis (Fig. 4, *E* and *F*). EPA reduced protein breakdown compared with both the vehicle and DHA treatments (Fig. 4*B*). No changes were detected in the level of ubiquitin-tagged proteins (Fig. 4, *D* and *F*).

EPA treatment differentially regulates DPA levels while DHA treatment differentially regulates AA levels. As previously mentioned, incubation of C₂C₁₂ with 50 μ M EPA or 50 μ M DHA led to substantial cellular incorporation of total omega-3 fatty acids (Fig. 1*A*). This was associated with the above mentioned physiological changes. To determine the potential mechanisms by which these effects occur, we deter-

mined via FAME analysis the fatty acid changes responsible for the increase in total n-3 levels in the cells treated with EPA/DHA. To clearly distinguish differential fatty acid shifts we presented the complete fatty acid profiles as fold-change (\log_2 ; Fig. 5). The most clearly differentiated fatty acid is DPA (22:5 n3), which demonstrates a significant $1,318 \pm 200\%$ increase with EPA treatment while DHA treatment induces a $17.83 \pm 17.37\%$ decrease in DPA content. Additionally, there is a trend ($P = 0.06$) for EPA treatment to increase the DHA content of the cells ($37.11 \pm 12.62\%$) suggesting that only a small proportion of the EPA is converted to DHA. Surprisingly, AA (20:4 n6) was only significantly decreased by DHA treatment ($-22.35 \pm 3.174\%$) and remained unaffected by EPA treatment. Intriguingly, we also observed that both EPA and DHA increased the content of the saturated fatty acid palmitate (PA, 16:0; Fig. 5). To build a more complete picture of the impact of EPA and DHA on the lipidome, we proceeded with a global lipidomics assessment.

Global lipidomics reveals that EPA and DHA treatments induce substantial divergence in the lipidome. Lipid extracts of cells treated with BSA (control), EPA, or DHA were analyzed by LC-MS in positive and negative ion modes, processed and subjected to multivariate data analysis. PCA highlights any natural clustering or separation within a data set and thereby enables similarities or differences between study groups to be explored. The PCA scores plots of both the positive and negative ion data sets revealed that EPA and DHA supplementation caused a substantial divergence in the lipidome, effectively segregating control and treated cells (Fig. 6, *A* and *B*). Having established the existence of clustering behavior be-

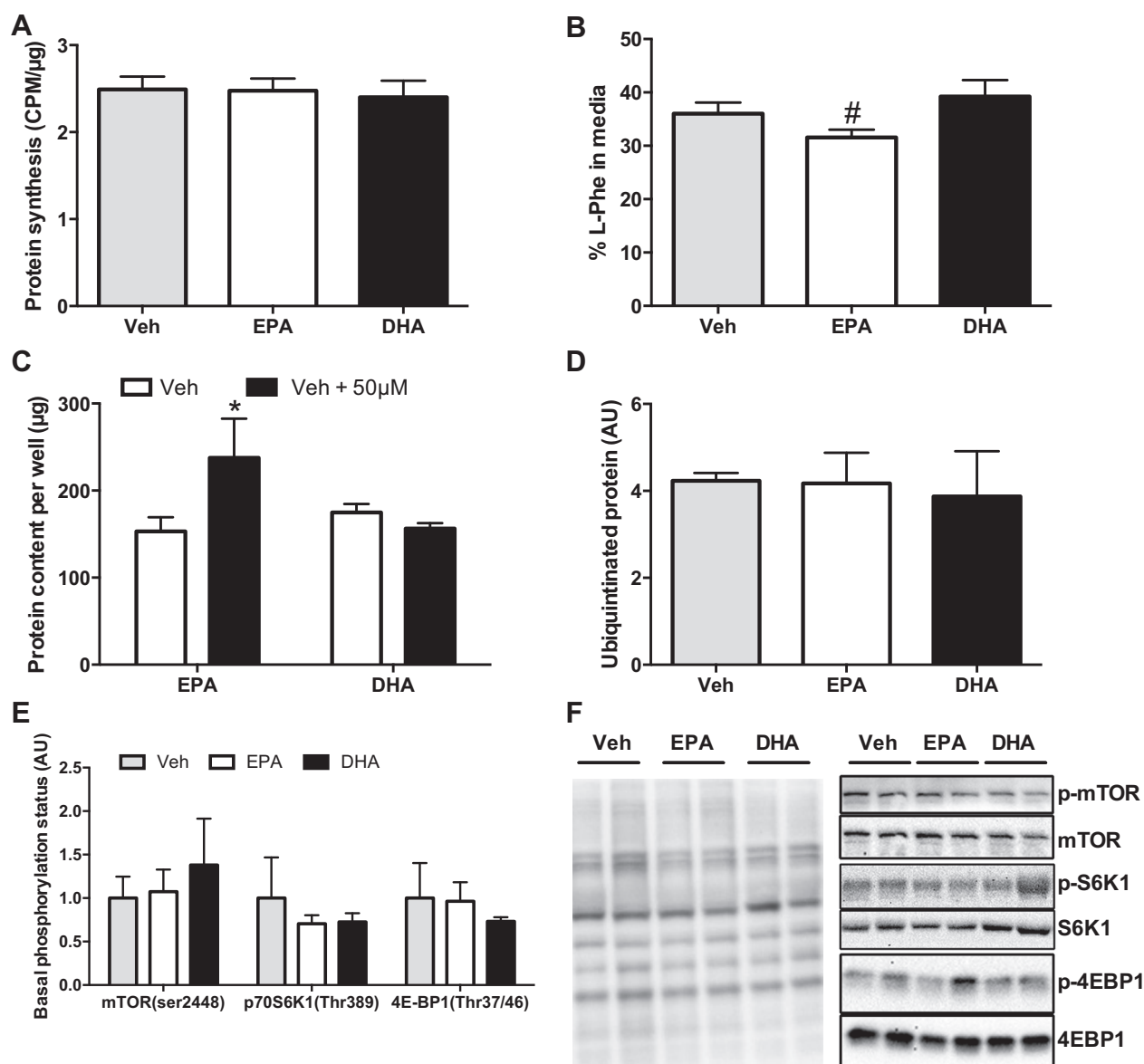


Fig. 4. EPA enhances protein accretion through a reduction in protein breakdown. *A*: protein synthesis was measured by a L-[2,4,³H]phenylalanine incorporation assay following a 24-h incubation with n-3 fatty acids ($n = 5$ in duplicate). *B*: protein breakdown was assessed by the release of L-[2,4,³H]phenylalanine into culture media after 24-h treatment with n-3 fatty acids ($n = 10$, in duplicate). *C*: total protein content was assessed after a 72-h incubation with EPA or DHA ($n = 5$, in duplicate). *D*: ubiquitination of proteins. *E*: phosphorylation of proteins within the mammalian target of rapamycin (mTOR) signaling pathway were assessed by Western blotting after a 24 h incubation with n-3 fatty acids ($n = 3$ in duplicate). *F*: ubiquitination of proteins was assessed by Western blotting after a 24-h incubation with fatty acids ($n = 3$ in duplicate). # $P < 0.05$, significantly different from vehicle and DHA. * $P < 0.05$, significantly different from corresponding control condition.

tween the sample cohorts, more powerful multivariate methods were used to characterize the specific lipid changes responsible for the observed shift in the lipidome of the EPA- and DHA-treated myotubes. The OPLS-DA score plots and associated "S" plots of the positive ion data are shown in Fig. 7, *A* and *B*. The results indicated that many of the key discriminating lipids associated with EPA and DHA treatment were phospholipids and in particular molecular species of PC and PE. In EPA-treated cells, elevations in PC and PE species containing both 20:5 and 22:5 fatty acids (in agreement with FAME analysis) were observed, whereas there were relative increases in the abundance of phospholipid species with a 22:6 fatty acid in DHA-treated cells. The analysis also revealed that both EPA

and DHA treatments also resulted in an elevation of PC 32:0, a saturated species. DHA was also found to be incorporated into a number of triglyceride species (see Supplemental Table S1; Supplemental Material for this article is available online at the Journal website). To fully understand the impact of EPA and DHA treatment, we followed up these experiments through the targeted analysis of the myotube phospholipids.

Targeted phospholipid analysis reveals that EPA and DHA increase the fraction of lipid species containing long chains and five or more double bonds at the expense of shorter chain, less saturated species. ESI-MS/MS was utilized to characterize the profiles of myocyte phospholipid classes. Representative mass spectra of PC and PE are shown in Fig. 8, *A* and *B*. The

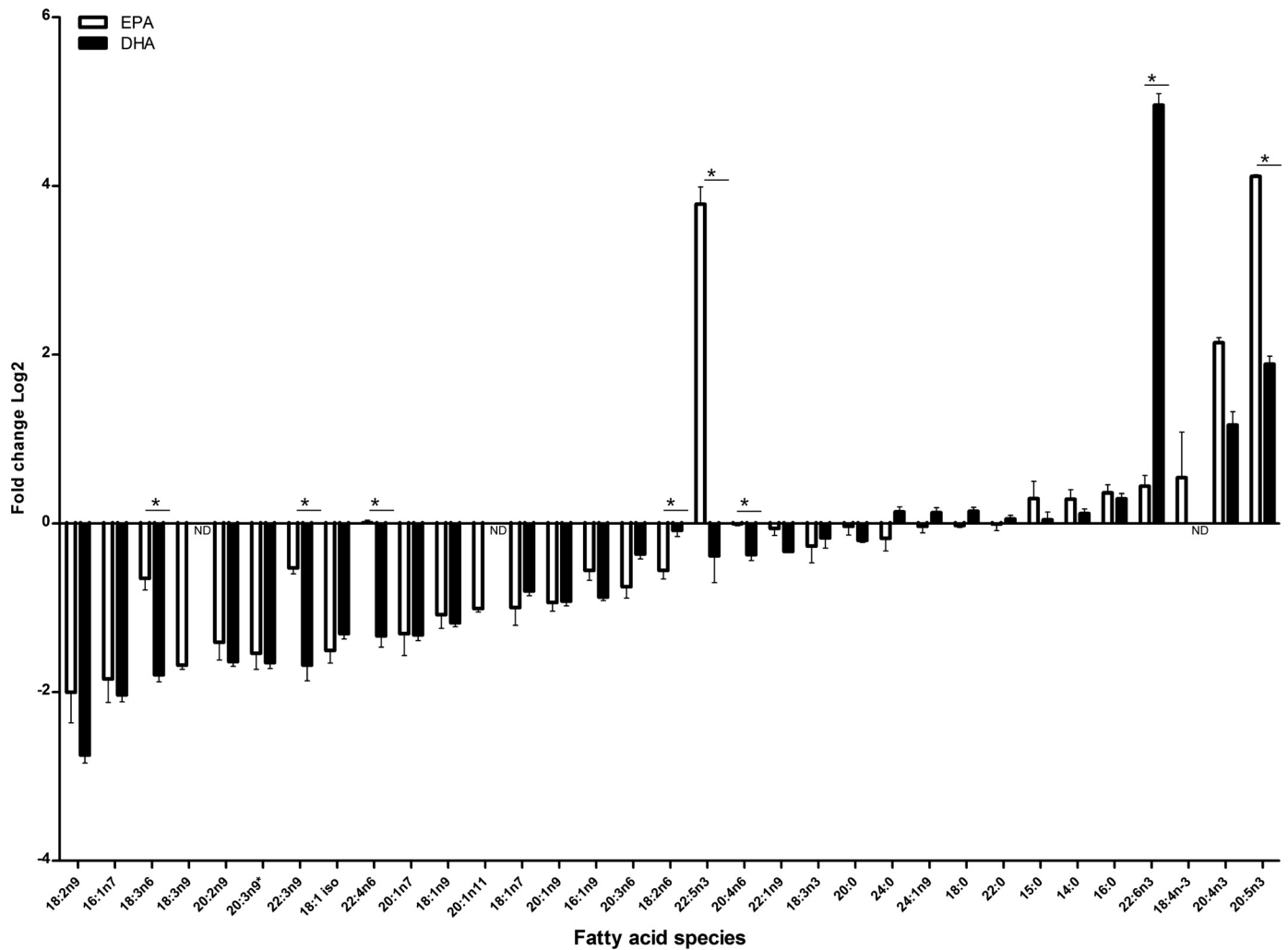


Fig. 5. Complete fatty acid profiles reveal a number of fatty acids differentially regulated by EPA and DHA. C₂C₁₂ myotubes were incubated in either 2% FAF-BSA or 2% FAF-BSA preconjugated to 50 μ M EPA or 50 μ M DHA for 72 h ($n = 4$ in duplicate). Cells were pelleted and washed 3 times using PBS with 2% FAF-BSA. Fatty acid analysis was carried out by FAME analysis. The fold-change was determined from the BSA control condition and logged (log₂). ND, nondetectable, * $P < 0.05$, significant difference between EPA vs. DHA.

general trends (Fig. 9) in both EPA and DHA were similar with the displacement of shorter chain in apparent preference for longer chain highly unsaturated fatty acids. However, the magnitude of change for these displacements was often higher with DHA. There was no evidence of alterations in the profile of sphingomyelin species in response to fatty acid treatments. ESI-MS/MS analysis of PS and PI was also performed; however, the low signal intensities of these lipids did not permit a robust quantification. Interestingly EPA and DHA supplementation led to a higher abundance of phospholipid species containing saturated fatty acids. For instance DHA induced an increase in PC (32:0) and LPE (16:0), while EPA induced an increase in PC (32:0), LPC (16:0; 18:0), and LPE (18:0). It is therefore evident that in spite of significant increases in saturated fatty acids in these EPA and DHA treatment still improve or maintain glucose uptake, respectively.

Altered composition of phospholipids is associated with altered membrane-associated proteomic profiles. As the lipidomic remodeling indicated substantial changes induced by n-3 treatment in the membrane-associated lipid species, we carried out SILAC based proteomics profiling of the membrane

fraction to assess if the lipid remodeling altered the proteins in the membrane fraction. Over 3,000 proteins associated with the membrane compartment were identified in the SILAC screen. These results were filtered down to 625 proteins (see Supplemental Table S1) with a coefficient of variance $\leq 5\%$ to describe consistent changes in membrane abundance. Proteins were considered enriched or reduced in the membrane with a fold change cut off of 0.25. Proteins similarly affected by EPA and DHA were removed from analysis. Proteins with altered abundance were then subject to gene ontology analysis for biological processes (see Supplemental Table S1). Membrane proteins altered by EPA were associated with protein folding ($P = 4.76E-03$). Additionally, these proteins were subjected to String analysis, which revealed that these proteins were highly likely to interact with each other (Fig. 10B). EPA also increased calumenin in the membrane fraction (1.34-fold). Interestingly, calumenin plays a role in calcium-sensitive protein folding (49). DHA altered proteins associated with a number of processes, primarily related to oxidative metabolism and ribosomal formation (see Supplemental Table S1). Further examination of ribosomal proteins revealed that DHA induced the

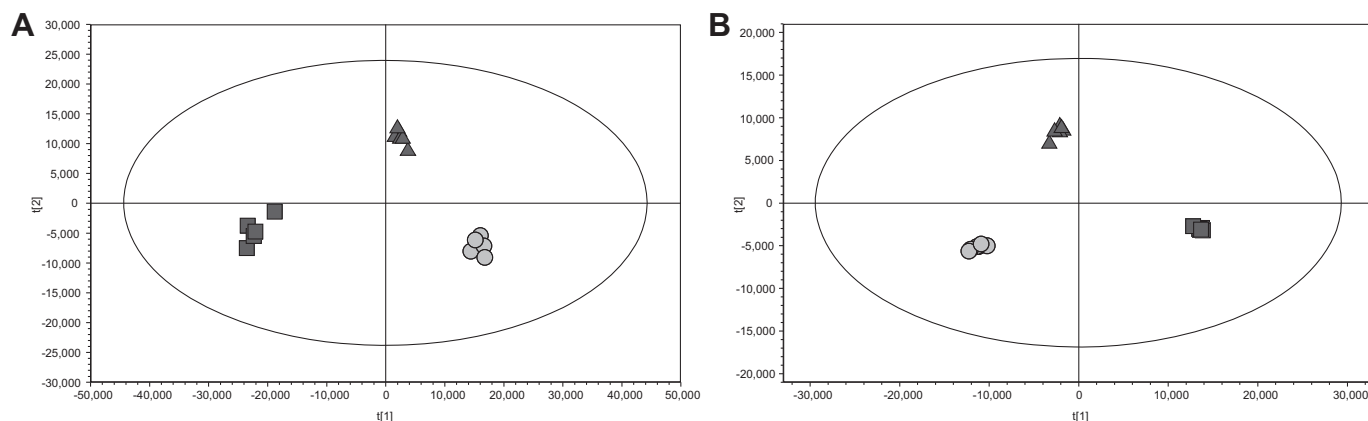


Fig. 6. Global lipidomic analysis characterizes shifts in lipid composition of C_2C_{12} myotubes. Principal component analysis (PCA) scores plots of lipid profiles generated by liquid chromatography-mass spectrometry (LC-MS) in positive ion (A) and negative ion modes (B). Cultured cells were incubated with either 2% FAF-BSA (circles) or 2% FAF-BSA preincubated to 50 μ M EPA (triangles) or 50 μ M DHA (squares) for 72 h. Global lipidomic analysis was performed on the cells, and the data sets were subjected to PCA with Pareto scaling. Each point represents a single cell sample ($n = 6$). The PCA revealed that the control, EPA, and DHA groups could be discriminated on the basis of their lipid profiles. The control cells were found to cluster in 1 area of the scores plot while cells treated with EPA or DHA appeared in regions away from the controls, indicating that there were alterations in their lipid composition as a result of the fatty acid treatments.

significant reduction in ribosomal proteins associated with both small and large subunits at the membrane (Fig. 10C). Conversely, EPA induced a small increase in ribosomal proteins (Fig. 10C).

DISCUSSION

This study is the first to carry out a comprehensive analysis of the lipidomic profiles of a skeletal muscle cell line in response to two differentially bioactive n-3 fatty acids. Furthermore, it is the first study, to our knowledge, to combine this with a profile of the membrane-associated proteome. We clearly demonstrate the differential metabolic activities of EPA vs. DHA in the C_2C_{12} skeletal muscle cell line and provide data demonstrating the differential impact that EPA and DHA have on the skeletal muscle lipidome. Our data suggest that the bioactivity of EPA may be due to its preferential incorporation (and possibly elongation to DPA) into the phospholipid fraction where it substantially alters the long-chain polyunsaturated fatty acid (PUFA) composition of major phospholipid classes. Likely secondary to the alterations in membrane-associated phospholipids we see an altered membrane-associated proteome. These changes in the membrane lipid-protein composition may be a key driver for the metabolic effects of n3 fatty acids.

Similar to previous cell culture-based studies (1, 21), we show that EPA has a positive effect on glucose uptake. Both basal and insulin-stimulated muscle glucose uptake were improved by EPA but not DHA. The increase in glucose uptake appears to be independent of changes in PKB signaling as measured by phosphorylation status, which suggests that enhanced proximal insulin and possibly PKB signaling are not part of the mechanism of action. Furthermore, there was no significant change to the expression of the glucose transporters GLUT1/4, hexokinase1/2, or the mitochondrial enzymes UQCRC2 and ATP-synthase, nor was there any significant change in mitochondrial function as assessed by the mitochondrial stress test. These data are difficult to consolidate; however, we hypothesize that the mechanism of action of EPA on

glucose uptake may be dependent less on changes in protein expression and more dependent on protein localization perhaps improving the functional coupling of glucose metabolism enzymes.

In addition to the EPA-induced improvements in glucose uptake, we also noted a significant improvement in protein accretion with EPA treatment, while DHA showed no significant effect. To determine the mechanism by which cells treated with EPA accumulate more protein, we assessed muscle protein synthesis and muscle protein breakdown. While Kamolrat and Gray (24) observed enhanced leucine-stimulated muscle protein synthetic response following EPA treatment, we detected no significant changes in basal muscle protein synthesis or the phosphorylation of anabolic signaling markers. Instead, we determined that the effect of EPA on protein accretion was likely driven by an \sim 10% reduction in muscle protein breakdown. Analysis of global ubiquitination via Western blotting indicates that the reduction in muscle protein breakdown may not be driven by a change in the activity of the ubiquitin system. Rather, it may be driven by reduced lysosomal degradation (9). In saying that, we must concede, however, that a 10% reduction in ubiquitin driven protein breakdown would be challenging to detect via Western blot analysis.

In an effort to determine the molecular mechanism of action of EPA on skeletal muscle glucose uptake and protein accretion, we tested the hypothesis that EPA and DHA treatments would induce significant lipid remodeling leading to remodeling of the cellular proteome. We found that while the total n-3 content was similar between treatments, EPA resulted in a larger variation in lipid species accumulating mainly as EPA and DPA and to a lesser extent DHA while DHA treatment mainly resulted in DHA accumulation with a decrease in DPA and a limited retro-conversion to EPA. The main differentially regulated fatty acids were DPA, increased in EPA and decreased in DHA, while only DHA decreased AA. Interestingly DPA accumulated to a similar extent as EPA (1,630% EPA vs. 1,318% DPA), findings consistent with previous literature in other tissues (2, 26). Given that DPA increased to a similar

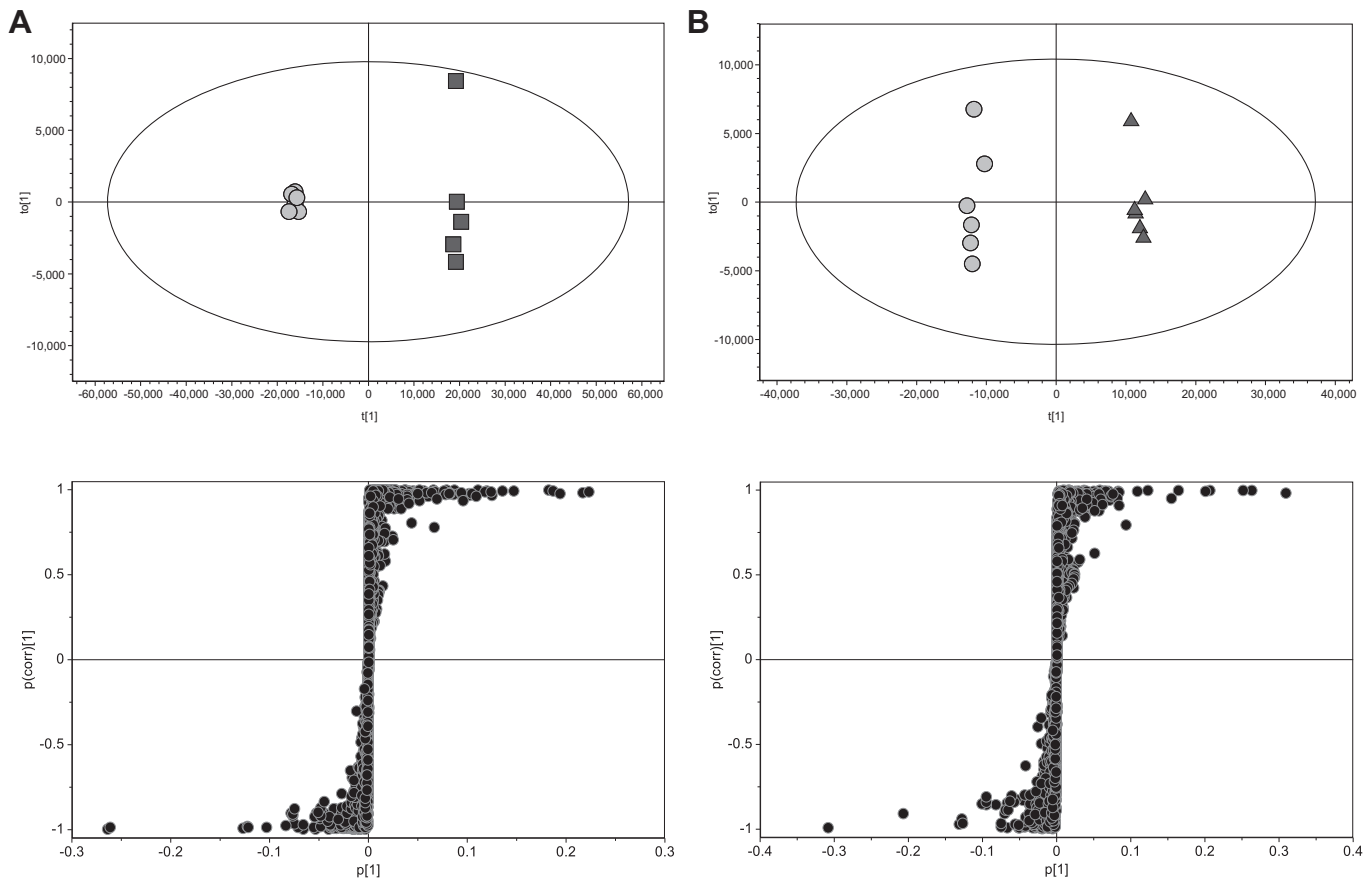


Fig. 7. Lipidomic profiling reveals cellular lipid species containing EPA, DPA, and DHA. Positive ion orthogonal partial least-squares discriminant analysis (OPLS-DA) for BSA vs. DHA (A) and BSA vs. EPA (B) ($n = 6$). Circles indicate BSA treated C_2C_{12} myotubes; squares indicate DHA-treated C_2C_{12} myotubes, and triangles indicate EPA-treated C_2C_{12} myotubes. The OPLS-DA scores plots indicated that EPA and DHA groups had distinct lipid profiles compared with the controls. To determine the lipids responsible for the interclass differences, associated S-plots of covariance vs. the correlation were generated. Each point in the S-plots represents a lipid detected in the LC-MS analysis with the lipids at the top and bottom of the plots showing the greatest changes. The analysis revealed that there was a relative increase in the abundance of lipid species containing 20:5, 22:5, or 22:6 fatty acids in EPA- and DHA-treated cells, respectively.

extent to EPA, we are unable to determine whether it is EPA or DPA that is the main driver behind the metabolic effects observed. These data suggest that upon intake into the cell EPA is elongated to DPA and to a lesser extent DHA. The elongation of EPA to DPA but not DHA may be explained by the differential affinities of the desaturases and elongases involved in fatty acid metabolism. In the n-3 pathway, *elovl2* catalyzes the conversion of EPA \rightarrow DPA \rightarrow 24:5 n-3, the precursor to DHA. However, increasing EPA concentrations is known to lower the saturation point in the conversion of DPA \rightarrow 24:5 n-3, which may play a role the accumulation of DPA without being further metabolized to DHA (19). Our data indicate that one of the primary fates of EPA and DHA was incorporation into the phospholipid fraction. In the global lipidomics screen, we found EPA- or DPA-containing lipid species associated with the phospholipid pool, while DHA-containing species were often associated with the TAG pool and EPA-containing species were rarely associated with the TAG pool (see Supplemental Table S1). Fatty acids in the TAG pool are stored in discrete lipid droplets and therefore may be less metabolically active than the phospholipids associated with the membranes. This differential incorporation into the various lipid pools may partially explain the beneficial metabolic effects of EPA.

The potential relevance of DPA as a mediator of many of the physiological effects of n-3 supplementation is beginning to be further understood. DPA more potently inhibits platelet aggregation than EPA or DHA (3) as well as more potently stimulating endothelial cell migration than EPA or DHA (25). In macrophages, EPA is a known inhibitor of the cyclooxygenase pathway and elongation to DPA is an important factor in this inhibition (36). We would suggest that the elongation of EPA to DPA seen in our study may also have important physiological roles in the increase in skeletal muscle glucose uptake by EPA. As with the global lipidomic analysis, we observed the incorporation of long-chain PUFAs into phospholipid species mainly at the expense of specific saturated fatty acids and monounsaturated fatty acids; however, some specific saturated fatty acids were increased by both EPA and DHA. We identified multiple differentially regulated phospholipid species across PE, PC, LPE, and LPC classes. In the EPA-treated group, a number of species were enriched by long-chain PUFAs with five or more double bonds in addition to a number of EPA- or DPA-containing phospholipids in the PC and PE, fractions. In comparison, the DHA-treated group increased the long-chain PUFA-containing phospholipids but did not increase or increase as much as EPA the content of species

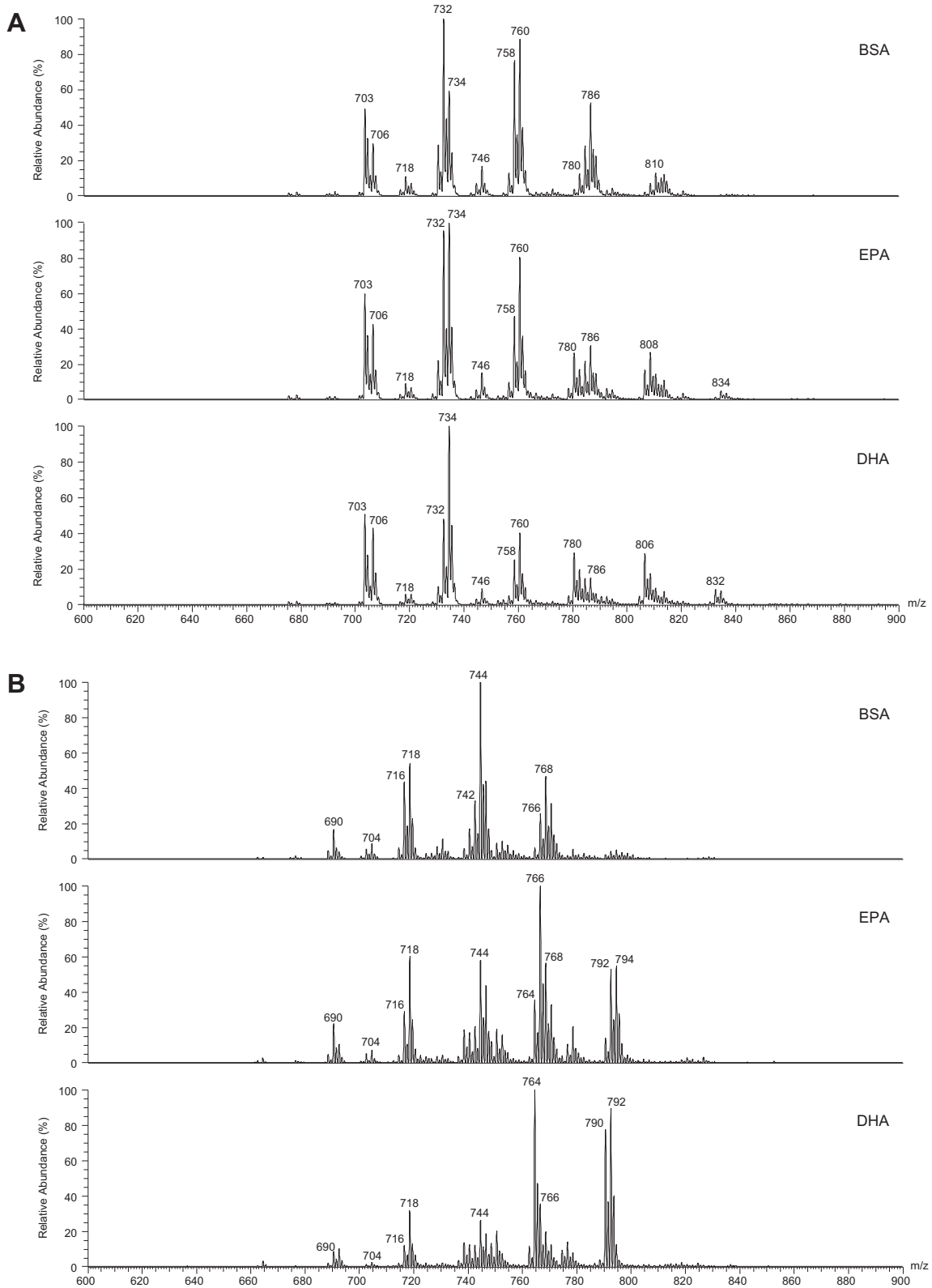


Fig. 8. Targeted phospholipid analysis indicates preferential incorporation of long-chain polyunsaturated fatty acids into specific phospholipid classes. C₂C₁₂ myotubes were solvent extracted and molecular species of phosphatidylcholine (A) and phosphatidylethanolamines (B) were detected by electrospray ionization-tandem mass spectrometry (ESI-MS/MS) in positive-ion mode by means of a precursor ion scan for m/z 184 and a neutral loss scan of m/z 141, respectively.

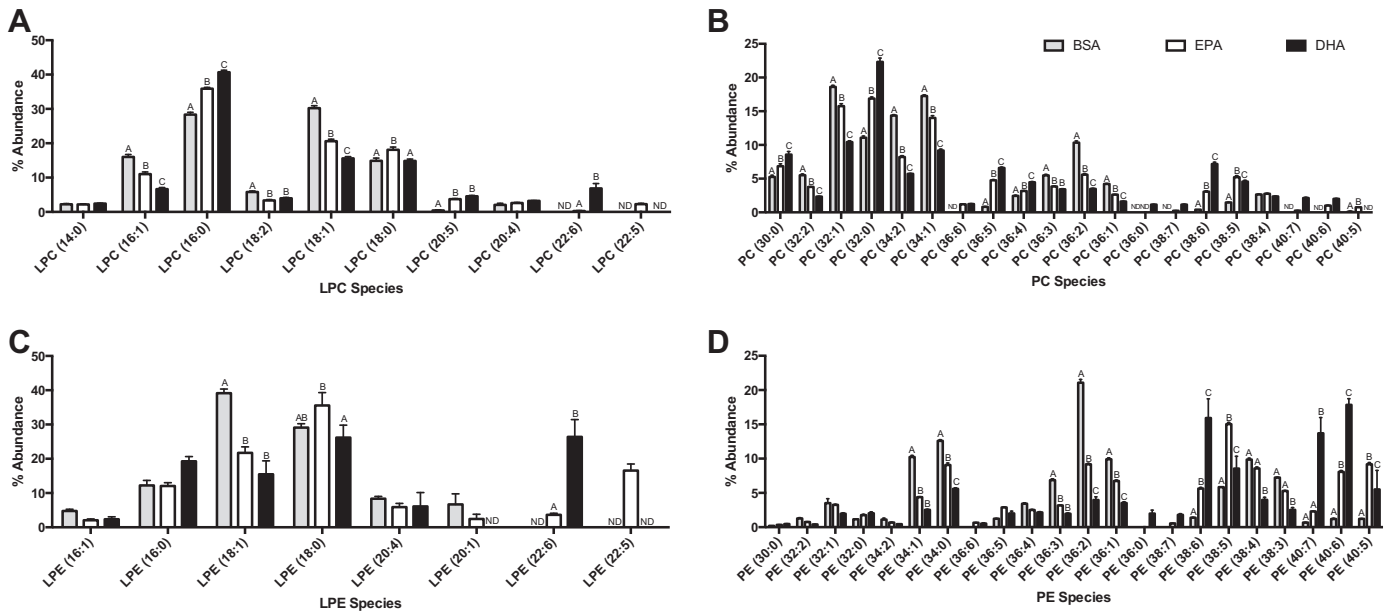


Fig. 9. Targeted phospholipid analysis presented as %abundance for phosphatidylcholine (PC), phosphatidylethanolamine (PE), lysophosphatidylcholine (LPC), and lysophosphatidylethanolamine (LPE) species. C_2C_{12} myotubes were solvent extracted, and molecular species of LPC (A), PC (B), LPE (C), and PE (D) were detected by ESI-MS/MS in positive-ion mode by means of a precursor ion scan for m/z 184 and a neutral loss scan of m/z 141, respectively. Data are presented as %abundance \pm SE. Bars not connected by the same letter are significantly different from one another ($P < 0.05$).

containing 22:5 or 40:5. Interestingly, with DHA treatment there was a trend for an increase in the palmitate containing lyso-PE content above that of control and EPA. Additionally, while it appears that many phospholipids containing saturated fatty acids are displaced in favor of polyunsaturated containing phospholipids, we observe a rise in PC (32:0) with both EPA and DHA, which may reflect the rise in palmitate observed with FAME analysis. Incorporation of PUFAs into phospholipids is known to increase membrane fluidity, and we speculate that this increase may be a compensatory mechanism to maintain a base level of membrane rigidity.

An attractive mechanism for the differential effects of EPA and DHA may lie in the reduced production of different inflammatory eicosanoids. However, only DHA reduced the total amount of AA. Additionally, the displacement of phospholipids alongside a lack of inflammatory stimulus suggests it is unlikely that this would mediate the metabolic differences seen in this model. The G protein-coupled receptor GPR120 has previously been identified as a general n-3 sensor in a number of tissues except skeletal muscle that elicits potent anti-inflammatory and consequently insulin-sensitizing effects (37). To our knowledge, no such receptor exists in skeletal muscle that can discriminate between EPA and DHA deeming it unlikely that the observed differential effects are mediated by EPA or DHA through specific receptor-activated signaling.

Phospholipid species are not merely inert structural components of cellular membranes, and their various roles in intracellular processes are beginning to be further understood. PS and PE are related phospholipid species found predominantly in the inner membrane and contribute to the membrane targeting and activation and modification of protein kinases (as reviewed in Ref. 51). It has also previously been seen that the lyso-PC, a hydrolyzed form of phospholipid, stimulated adipocyte glucose uptake in a manner dependent on chain length and saturation of the acyl group (54). We observed an incor-

poration of long-chain PUFAs (possibly EPA and DPA) into the PC, PS, PE, and certain lyso-phospholipid species and therefore cannot discount that the change in acyl chain length and unsaturation level alters the function of these phospholipid species and leads to an increase in glucose uptake through a currently unknown mechanism. Because the lipid composition of the membrane can alter the targeting of various proteins to the membrane (50, 51), we speculated that part of the mechanism of action of EPA might be via a change in the composition of the membrane-associated proteome. To test this theory, we carried out a three-way SILAC experiment on the membrane fractions of cells treated with vehicle, EPA, or DHA.

Our SILAC experiment illustrated the proof of concept that the incorporation of EPA and DHA into phospholipid species was associated with the alteration of proteins interacting with the membrane compartment. There are a number of mechanisms by which proteins can bind to the membrane that are influenced by the fatty acid composition of the lipid bilayers (50, 51). Gene ontology analysis indicated that proteins associated with protein folding at the membrane were overrepresented following EPA incorporation. There is experimental evidence that a number of the proteins identified with this process interact, as probed by the STRING database. Furthermore, analysis of ribosomal proteins indicated a small but significant shift of ribosomal proteins toward the membrane fraction in EPA-treated cells. Since the endoplasmic reticulum (ER) is a membranous structure, these data suggest that EPA is increasing the content of ribosomes at the ER. This shift in ribosomes toward the ER could lead to improved fidelity of protein production as the ER is key to protein quality control (15). We propose a mechanism in which protein folding is enhanced, thereby enhancing the fidelity with which proteins are synthesized, thereby reducing protein breakdown leading to increased protein accretion. Further experimental work is needed to confirm this hypothesis since misfolded proteins tend

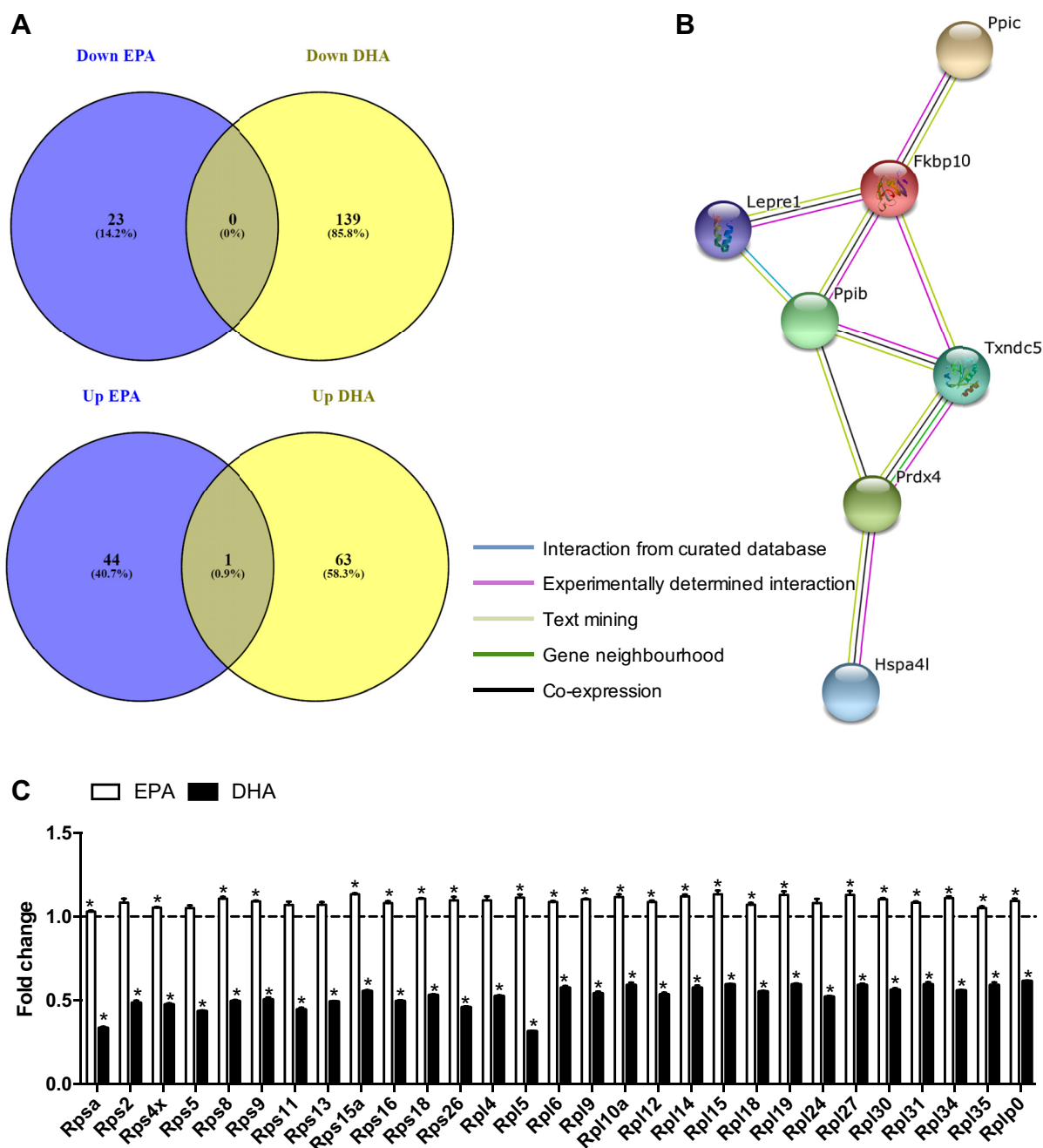


Fig. 10. Membrane-associated proteomics reveals protein folding machinery and ribosomal proteins differentially shift to the membrane in response to EPA treatment. C_2C_{12} myotubes were incubated in stable isotope labeling by amino acids in cell culture (SILAC) media for 7 doublings followed by plating and differentiation for 72 h in SILAC differentiation media. Following differentiation myotubes were incubated in either 2% FAF-BSA or 2% FAF-BSA pre-conjugated to 50 μ M EPA or 50 μ M DHA for 72 h ($n = 3$ in duplicate). Cells were collected and fractionated, and the membrane fraction was then submitted to proteomics analysis. *A*: Venn diagram illustrating the number of proteins found to be changed in the membrane fraction in response to EPA/DHA. *B*: String diagram illustrating the interactions between the proteins identified from the gene ontology analysis as being involved in “protein folding.” *C*: fold-change in ribosomal proteins in the membrane fraction in response to EPA/DHA. All differences between EPA and DHA were significant. * $P < 0.05$, significant fold-change from control.

to be degraded by the ubiquitin-proteasome system (9) and our data indicated that global ubiquitination was not reduced by EPA. By comparison, DHA caused a striking reduction in the abundance of a number of ribosomal proteins with the membrane fraction. If future work confirms that total ribosomal content is unchanged with these conditions, then these data would indicate an increase in cytosolic ribosomes. This differ-

ential shift in ribosomal compartmentalization may indicate a shift in protein expression profiles. Proteins that enter the secretory pathways or integral membrane proteins are synthesized in the ER while other proteins are translated in the cytosolic ribosome pool (41).

DHA also altered the abundance of proteins involved in ATP-coupled proton transport and acetyl-CoA metabolism.

The proteins identified with ATP synthesis-coupled transport were mainly downregulated proteins in the ATP synthase complex. This would be expected to manifest as a reduced ability to generate ATP, yet no changes were observed in ATP synthase-dependent oxygen consumption. The effects of DHA may not have been severe enough to observe at basal levels. Although maximal respiration is measured during the mitostress test, it is induced by uncoupling so may not be indicative of changes in ATP synthesis. Previous studies have observed that omega-3 fatty acids can alter mitochondrial function, altering ADP kinetics without altering maximal respiration (20). It remains to be seen if this reduction in ATP synthase proteins would alter the mitochondrial response to cellular stress or changing substrate availability.

In summary, we demonstrate that EPA and DHA display divergent metabolic activities in a skeletal muscle cell line, which may be partially mediated by differential remodeling of the lipidome. We speculate that the remodeling of the membrane-associated proteome is secondary to the changes observed in the saturation profile of the membrane-associated phospholipid species. While the proteomic data did not reveal a mechanism for the effects of EPA on glucose uptake, our data support the proof of concept that a redistribution of the proteome may be responsible. Gene ontology analysis of the proteomic data indicates that the mechanism of action of EPA on protein metabolism may be driven by an improved fidelity with which proteins are synthesized. Based on the shifts in ribosomal proteins found in the membrane fractions, future work should determine whether EPA and DHA alter the transcript profiles in various ribosomal fractions.

ACKNOWLEDGMENTS

We acknowledge Liz Mackinlay for assistance with the FAME analysis.

GRANTS

This work was funded by a University of Stirling capital investment award (to D. L. Hamilton) and Society for Endocrinology and American College of Sports Medicine early career awards (to D. L. Hamilton). The financial support of Highlands and Islands Enterprise, the Scottish Funding Council, and European Regional Development Fund is gratefully acknowledged (to I. Mackenzie, M. K. Doherty, and P. D. Whitfield).

DISCLOSURES

A number of the authors have received funding or hold funding from various segments of the aquaculture industry. This funding is to perform research, and none of that research contributed to this manuscript.

AUTHOR CONTRIBUTIONS

S.G., I.G., and D.L.H. conceived and designed research; S.J., I.M., M.K.D., A.S., S.A., and D.L.H. performed experiments; S.J., I.M., M.K.D., P.D.W., G.B., J.D., A.S., F.R., S.A., A.P., S.G., I.G., and D.L.H. analyzed data; S.J., M.K.D., P.D.W., G.B., J.D., F.R., A.P., S.G., I.G., and D.L.H. interpreted results of experiments; S.J., P.D.W., I.G., and D.L.H. prepared figures; D.L.H. drafted manuscript; S.J., M.K.D., P.D.W., F.R., A.P., and D.L.H. edited and revised manuscript; S.J., I.M., M.K.D., P.D.W., G.B., J.D., A.S., F.R., S.A., A.P., S.G., I.G., and D.L.H. approved final version of manuscript.

REFERENCES

1. Aas V, Rokling-Andersen MH, Kase ET, Thoresen GH, Rustan AC. Eicosapentaenoic acid (20:5 n-3) increases fatty acid and glucose uptake in cultured human skeletal muscle cells. *J Lipid Res* 47: 366–374, 2006. doi:10.1194/jlr.M500300-JLR200.
2. Achard F, Bénistant C, Lagarde M. Interconversions and distinct metabolic fate of eicosapentaenoic, docosapentaenoic and docosahexaenoic

- acids in bovine aortic endothelial cells. *Biochim Biophys Acta* 1255: 260–266, 1995. doi:10.1016/0005-2760(94)00238-T.
- 2a. Ackman RG. Fish lipids, part I. In: *Advances in Fish Science and Technology*, edited by J. J. Connell. Farnham Surrey, UK: Fishing News Books, 1980 p. 86–103.
3. Akiba S, Murata T, Kitatani K, Sato T. Involvement of lipoxygenase pathway in docosapentaenoic acid-induced inhibition of platelet aggregation. *Biol Pharm Bull* 23: 1293–1297, 2000. doi:10.1248/bpb.23.1293.
4. Akinkuolie AO, Ngwa JS, Meigs JB, Djoussé L. Omega-3 polyunsaturated fatty acid and insulin sensitivity: a meta-analysis of randomized controlled trials. *Clin Nutr* 30: 702–707, 2011. doi:10.1016/j.clnu.2011.08.013.
5. Alexander JW, Saito H, Trocki O, Ogle CK. The importance of lipid type in the diet after burn injury. *Ann Surg* 204: 1–8, 1986. doi:10.1097/0000658-198607000-00001.
6. Andersson A, Näslén C, Tengblad S, Vessby B. Fatty acid composition of skeletal muscle reflects dietary fat composition in humans. *Am J Clin Nutr* 76: 1222–1229, 2002.
7. Browning LM, Walker CG, Mander AP, West AL, Gambell J, Madden J, Calder PC, Jebb SA. Compared with daily, weekly n-3 PUFA intake affects the incorporation of eicosapentaenoic acid and docosahexaenoic acid into platelets and mononuclear cells in humans. *J Nutr* 144: 667–672, 2014. doi:10.3945/jn.113.186346.
8. Burdge GC, Calder PC. Introduction to fatty acids and lipids. *World Rev Nutr Diet* 112: 1–16, 2015.
- 8a. Christie WW. Preparation of derivatives of fatty acids for chromatographic analysis. In: *Advances in Lipid Methodology 2*, edited by W. W. Christie. Bridgwater, UK: Oily Press, 1993 p. 69–111.
9. Ciechanover A. Intracellular protein degradation: from a vague idea thru the lysosome and the ubiquitin-proteasome system and onto human diseases and drug targeting. *Cell Death Differ* 12: 1178–1190, 2005. doi:10.1038/sj.cdd.4401692.
10. Cox J, Mann M. MaxQuant enables high peptide identification rates, individualized p.p.b.-range mass accuracies and proteome-wide protein quantification. *Nat Biotechnol* 26: 1367–1372, 2008. doi:10.1038/nbt.1511.
11. Cox J, Neuhauser N, Michalski A, Scheltema RA, Olsen JV, Mann M. Andromeda: a peptide search engine integrated into the MaxQuant environment. *J Proteome Res* 10: 1794–1805, 2011. doi:10.1021/pr101065j.
12. Da Boit M, Sibson R, Sivasubramaniam S, Meakin JR, Greig CA, Aspden RM, Thies F, Jeromson S, Hamilton DL, Speakman JR, Hambly C, Mangoni AA, Preston T, Gray SR. Sex differences in the effect of fish oil supplementation on the adaptive response to resistance exercise training in older people: a randomized control trial. *Am J Clin Nutr*, 2016.
13. Dangardt F, Chen Y, Gronowitz E, Dahlgren J, Friberg P, Strandvik B. High physiological omega-3 fatty acid supplementation affects muscle fatty acid composition and glucose and insulin homeostasis in obese adolescents. *J Nutr Metab* 2012: 395757, 2012. doi:10.1155/2012/395757.
14. Di Girolamo FG, Situlin R, Mazzucco S, Valentini R, Toigo G, Biolo G. Omega-3 fatty acids and protein metabolism: enhancement of anabolic interventions for sarcopenia. *Curr Opin Clin Nutr Metab Care* 17: 145–150, 2014. doi:10.1097/MCO.000000000000032.
15. Ellgaard L, Helenius A. Quality control in the endoplasmic reticulum. *Nat Rev Mol Cell Biol* 4: 181–191, 2003. doi:10.1038/nrm1052.
16. Findlay JA, Hamilton DL, Ashford ML. BACE1 activity impairs neuronal glucose oxidation: rescue by beta-hydroxybutyrate and lipoic acid. *Front Cell Neurosci* 9: 382, 2015. doi:10.3389/fncel.2015.00382.
17. Folch J, Lees M, Sloane Stanley GH. A simple method for the isolation and purification of total lipides from animal tissues. *J Biol Chem* 226: 497–509, 1957.
18. Franekova V, Angin Y, Hoebbers NT, Coumans WA, Simons PJ, Glatz JF, Luiken JJ, Larsen TS. Marine omega-3 fatty acids prevent myocardial insulin resistance and metabolic remodeling as induced experimentally by high insulin exposure. *Am J Physiol Cell Physiol* 308: C297–C307, 2015. doi:10.1152/ajpcell.00073.2014.
- 18a. Ghioni C, Bell JG, Sargent JR. Polyunsaturated fattyacids in neutral lipids and phospholipids of some freshwater insects. *Comp Biochem Physiol* 114B: 161–170, 1996.
19. Gregory MK, Gibson RA, Cook-Johnson RJ, Cleland LG, James MJ. Elongase reactions as control points in long-chain polyunsaturated fatty acid synthesis. *PLoS One* 6: e29662, 2011. doi:10.1371/journal.pone.0029662.

20. Herbst EA, Pagliarunga S, Gerling C, Whitfield J, Mukai K, Chabowski A, Heigenhauser GJ, Spriet LL, Holloway GP. Omega-3 supplementation alters mitochondrial membrane composition and respiration kinetics in human skeletal muscle. *J Physiol* 592: 1341–1352, 2014. doi:10.1113/jphysiol.2013.267336.
21. Hessvik NP, Bakke SS, Fredriksson K, Boekschoten MV, Fjørkenstad A, Koster G, Hesselink MK, Kersten S, Kase ET, Rustan AC, Thoresen GH. Metabolic switching of human myotubes is improved by n-3 fatty acids. *J Lipid Res* 51: 2090–2104, 2010. doi:10.1194/jlr.M003319.
22. Huang F, Wei H, Luo H, Jiang S, Peng J. EPA inhibits the inhibitor of κB ($\text{I}\kappa\text{B}$)/NF- κB /muscle RING finger 1 pathway in C2C12 myotubes in a PPAR γ -dependent manner. *Br J Nutr* 105: 348–356, 2011. doi:10.1017/S0007114510003703.
23. Jucker BM, Cline GW, Barucci N, Shulman GI. Differential effects of safflower oil versus fish oil feeding on insulin-stimulated glycogen synthesis, glycolysis, and pyruvate dehydrogenase flux in skeletal muscle: a ^{13}C nuclear magnetic resonance study. *Diabetes* 48: 134–140, 1999. doi:10.2337/diabetes.48.1.134.
24. Kamolrat T, Gray SR. The effect of eicosapentaenoic and docosahexaenoic acid on protein synthesis and breakdown in murine C2C12 myotubes. *Biochem Biophys Res Commun* 432: 593–598, 2013. doi:10.1016/j.bbrc.2013.02.041.
25. Kanayasu-Toyoda T, Morita I, Murota S. Docosapentaenoic acid (22:5, n-3), an elongation metabolite of eicosapentaenoic acid (20:5, n-3), is a potent stimulator of endothelial cell migration on pretreatment in vitro. *Prostaglandins Leukot Essent Fatty Acids* 54: 319–325, 1996. doi:10.1016/S0952-3278(96)90045-9.
26. Kaur G, Sinclair AJ, Cameron-Smith D, Barr DP, Molero-Navajas JC, Konstantopoulos N. Docosapentaenoic acid (22:5n-3) down-regulates the expression of genes involved in fat synthesis in liver cells. *Prostaglandins Leukot Essent Fatty Acids* 85: 155–161, 2011. doi:10.1016/j.plefa.2011.06.002.
27. Lamaziere A, Wolf C, Barbe U, Bausero P, Visioli F. Lipidomics of hepatic lipogenesis inhibition by omega 3 fatty acids. *Prostaglandins Leukot Essent Fatty Acids* 88: 149–154, 2013. doi:10.1016/j.plefa.2012.12.001.
28. Lanza IR, Blachnio-Zabielska A, Johnson ML, Schimke JM, Jakaitis DR, Lebrasseur NK, Jensen MD, Sreekumaran Nair K, Zabielski P. Influence of fish oil on skeletal muscle mitochondrial energetics and lipid metabolites during high-fat diet. *Am J Physiol Endocrinol Metab* 304: E1391–E1403, 2013. doi:10.1152/ajpendo.00584.2012.
29. Magee P, Pearson S, Whittingham-Dowd J, Allen J. PPAR γ as a molecular target of EPA anti-inflammatory activity during TNF- α -impaired skeletal muscle cell differentiation. *J Nutr Biochem* 23: 1440–1448, 2012. doi:10.1016/j.jnutbio.2011.09.005.
30. McGlory C, Galloway SD, Hamilton DL, McClintock C, Breen L, Dick JR, Bell JG, Tipton KD. Temporal changes in human skeletal muscle and blood lipid composition with fish oil supplementation. *Prostaglandins Leukot Essent Fatty Acids* 90: 199–206, 2014. doi:10.1016/j.plefa.2014.03.001.
31. Mori TA, Burke V, Puddey IB, Watts GF, O'Neal DN, Best JD, Beilin LJ. Purified eicosapentaenoic and docosahexaenoic acids have differential effects on serum lipids and lipoproteins, LDL particle size, glucose, and insulin in mildly hyperlipidemic men. *Am J Clin Nutr* 71: 1085–1094, 2000.
32. Mori TA, Codde JP, Vandongen R, Beilin LJ. New findings in the fatty acid composition of individual platelet phospholipids in man after dietary fish oil supplementation. *Lipids* 22: 744–750, 1987. doi:10.1007/BF02533975.
33. Morisaki N, Kanzaki T, Fujiyama Y, Osawa I, Shirai K, Matsuoka N, Saito Y, Yoshida S. Metabolism of n-3 polyunsaturated fatty acids and modification of phospholipids in cultured rabbit aortic smooth muscle cells. *J Lipid Res* 26: 930–939, 1985.
34. Murphy RA, Mourtzakis M, Mazurak VC. n-3 polyunsaturated fatty acids: the potential role for supplementation in cancer. *Curr Opin Clin Nutr Metab Care* 15: 246–251, 2012. doi:10.1097/MCO.0b013e328351c32f.
35. Neschen S, Morino K, Dong J, Wang-Fischer Y, Cline GW, Romanelli AJ, Rossbacher JC, Moore IK, Regittinig W, Munoz DS, Kim JH, Shulman GI. n-3 Fatty acids preserve insulin sensitivity in vivo in a peroxisome proliferator-activated receptor- α -dependent manner. *Diabetes* 56: 1034–1041, 2007. doi:10.2337/db06-1206.
36. Norris PC, Dennis EA. Omega-3 fatty acids cause dramatic changes in TLR4 and purinergic eicosanoid signaling. *Proc Natl Acad Sci USA* 109: 8517–8522, 2012. doi:10.1073/pnas.1200189109.
37. Oh DY, Talukdar S, Bae EJ, Imamura T, Morinaga H, Fan W, Li P, Lu WJ, Watkins SM, Olefsky JM. GPR120 is an omega-3 fatty acid receptor mediating potent anti-inflammatory and insulin-sensitizing effects. *Cell* 142: 687–698, 2010. doi:10.1016/j.cell.2010.07.041.
38. Ong SE, Blagoev B, Kratchmarova I, Kristensen DB, Steen H, Pandey A, Mann M. Stable isotope labeling by amino acids in cell culture, SILAC, as a simple and accurate approach to expression proteomics. *Mol Cell Proteomics* 1: 376–386, 2002. doi:10.1074/mcp.M200025-MCP200.
39. Ries A, Trottenberg P, Elsner F, Stiel S, Haugen D, Kaasa S, Radbruch L. A systematic review on the role of fish oil for the treatment of cachexia in advanced cancer: an EPCRC cachexia guidelines project. *Palliat Med* 26: 294–304, 2012. doi:10.1177/0269216311418709.
40. Rodacki CL, Rodacki AL, Pereira G, Naliwaiko K, Coelho I, Pequito D, Fernandes LC. Fish-oil supplementation enhances the effects of strength training in elderly women. *Am J Clin Nutr* 95: 428–436, 2012. doi:10.3945/ajcn.111.021915.
41. Ron D. Translational control in the endoplasmic reticulum stress response. *J Clin Invest* 110: 1383–1388, 2002. doi:10.1172/JCI0216784.
42. Sjövall P, Rossmel M, Hanrieder J, Kuda O, Kopecky J, Bryhn M. Dietary uptake of omega-3 fatty acids in mouse tissue studied by time-of-flight secondary ion mass spectrometry (TOF-SIMS). *Anal Bioanal Chem* 407: 5101–5111, 2015. doi:10.1007/s00216-015-8515-7.
43. Smith GI, Atherton P, Reeds DN, Mohammed BS, Rankin D, Rennie MJ, Mittendorfer B. Dietary omega-3 fatty acid supplementation increases the rate of muscle protein synthesis in older adults: a randomized controlled trial. *Am J Clin Nutr* 93: 402–412, 2011. doi:10.3945/ajcn.110.005611.
44. Smith GI, Atherton P, Reeds DN, Mohammed BS, Rankin D, Rennie MJ, Mittendorfer B. Omega-3 polyunsaturated fatty acids augment the muscle protein anabolic response to hyperinsulinaemia-hyperaminoacidaemia in healthy young and middle-aged men and women. *Clin Sci (Lond)* 121: 267–278, 2011. doi:10.1042/CS20100597.
45. Smith GI, Julliard S, Reeds DN, Sinacore DR, Klein S, Mittendorfer B. Fish oil-derived n-3 PUFA therapy increases muscle mass and function in healthy older adults. *Am J Clin Nutr* 102: 115–122, 2015. doi:10.3945/ajcn.114.105833.
46. Stephens FB, Mendis B, Shannon CE, Cooper S, Ortori CA, Barrett DA, Mansell P, Tsintzas K. Fish oil omega-3 fatty acids partially prevent lipid-induced insulin resistance in human skeletal muscle without limiting acylcarnitine accumulation. *Clin Sci (Lond)* 127: 315–322, 2014. doi:10.1042/CS20140031.
47. Storlien LH, Jenkins AB, Chisholm DJ, Pascoe WS, Khouri S, Kraegen EW. Influence of dietary fat composition on development of insulin resistance in rats. Relationship to muscle triglyceride and omega-3 fatty acids in muscle phospholipid. *Diabetes* 40: 280–289, 1991. doi:10.2337/diab.40.2.280.
48. Storlien LH, Kraegen EW, Chisholm DJ, Ford GL, Bruce DG, Pascoe WS. Fish oil prevents insulin resistance induced by high-fat feeding in rats. *Science* 237: 885–888, 1987. doi:10.1126/science.3303333.
49. Tripathi R, Benz N, Culetton B, Trouné P, Férec C. Biophysical characterisation of calumenin as a charged F508del-CFTR folding modulator. *PLoS One* 9: e104970, 2014. doi:10.1371/journal.pone.0104970.
50. Vance JE. Phospholipid synthesis and transport in mammalian cells. *Traffic* 16: 1–18, 2015. doi:10.1111/tra.12230.
51. Vance JE, Tasseva G. Formation and function of phosphatidylserine and phosphatidylethanolamine in mammalian cells. *Biochim Biophys Acta* 1831: 543–554, 2013. doi:10.1016/j.bbalip.2012.08.016.
52. Wang Y, Lin QW, Zheng PP, Zhang JS, Huang FR. DHA inhibits protein degradation more efficiently than EPA by regulating the PPAR γ /NF κB pathway in C2C12 myotubes. *Biomed Res Int* 2013: 318981, 2013. doi:10.1155/2013/318981.
53. Woodman RJ, Mori TA, Burke V, Puddey IB, Watts GF, Best JD, Beilin LJ. Docosahexaenoic acid but not eicosapentaenoic acid increases LDL particle size in treated hypertensive type 2 diabetic patients. *Diabetes Care* 26: 253, 2003. doi:10.2337/diacare.26.1.253.
54. Yea K, Kim J, Yoon JH, Kwon T, Kim JH, Lee BD, Lee HJ, Lee SJ, Kim JI, Lee TG, Baek MC, Park HS, Park KS, Ohba M, Suh PG, Ryu SH. Lysophosphatidylcholine activates adipocyte glucose uptake and lowers blood glucose levels in murine models of diabetes. *J Biol Chem* 284: 33833–33840, 2009. doi:10.1074/jbc.M109.024869.
55. You JS, Park MN, Song W, Lee YS. Dietary fish oil alleviates soleus atrophy during immobilization in association with Akt signaling to p70s6k and E3 ubiquitin ligases in rats. *Appl Physiol Nutr Metab* 35: 310–318, 2010. doi:10.1139/H10-022.